



Evaluation of Lung Aeration and Respiratory System Mechanics in Obese Dogs Ventilated With Tidal Volumes Based on Ideal vs. Current Body Weight

Joaquin Araos^{1*}, Luca Lacitignola², Valentina de Monte², Marzia Stabile², Ian Porter¹, Daniel E. Hurtado^{3,4,5}, Agustín Perez⁴, Antonio Crovace², Salvatore Grasso⁶, Manuel Martin-Flores¹ and Francesco Staffieri²

OPEN ACCESS

Edited by:

Aline Magalhães Magalhães
Ambrósio,
University of São Paulo, Brazil

Reviewed by:

Joao Henrique Neves Soares,
University of California, Davis,
United States

Celine Pouzot-Nevoret,
VetAgro Sup, France

*Correspondence:

Joaquin Araos
jda246@cornell.edu

Specialty section:

This article was submitted to
Veterinary Emergency and Critical
Care Medicine,
a section of the journal
Frontiers in Veterinary Science

Received: 04 May 2021

Accepted: 06 September 2021

Published: 01 October 2021

Citation:

Araos J, Lacitignola L, de Monte V,
Stabile M, Porter I, Hurtado DE,
Perez A, Crovace A, Grasso S,
Martin-Flores M and Staffieri F (2021)
Evaluation of Lung Aeration and
Respiratory System Mechanics in
Obese Dogs Ventilated With Tidal
Volumes Based on Ideal vs. Current
Body Weight.
Front. Vet. Sci. 8:704863.
doi: 10.3389/fvets.2021.704863

¹ Department of Clinical Sciences, College of Veterinary Medicine, Cornell University, Ithaca, NY, United States, ² Section of Veterinary Clinics and Animal Production, Department of Emergency and Organ Transplantation D.E.O.T., "Aldo Moro" University of Bari, Bari, Italy, ³ Department of Structural and Geotechnical Engineering, School of Engineering, Pontificia Universidad Católica de Chile, Santiago, Chile, ⁴ Institute for Biological and Medical Engineering, Schools of Engineering, Medicine and Biological Sciences, Pontificia Universidad Católica de Chile, Santiago, Chile, ⁵ Millennium Nucleus for Cardiovascular Magnetic Resonance, Santiago, Chile, ⁶ Section of Anesthesia and Intensive Care, Department of Emergency and Organ Transplantation D.E.O.T., "Aldo Moro" University of Bari, Bari, Italy

We describe the respiratory mechanics and lung aeration in anesthetized obese dogs ventilated with tidal volumes (VT) based on ideal (VTi) vs. current (VTc) body weight. Six dogs with body condition scores $\geq 8/9$ were included. End-expiratory respiratory mechanics and end-expiratory CT-scan were obtained at baseline for each dog. Thereafter, dogs were ventilated with VT 15 ml kg⁻¹ based on VTi and VTc, applied randomly. Respiratory mechanics and CT-scan were repeated at end-inspiration during VTi and VTc. Data analyzed with linear mixed models and reported as mean \pm SD or median [range]. Statistical significance $p < 0.05$. The elastance of the lung, chest wall and respiratory system indexed by ideal body weight (IBW) were positively correlated with body fat percentage, whereas the functional residual capacity indexed by IBW was negatively correlated with body fat percentage. At end-expiration, aeration (%) was: hyperaeration 0.03 [0.00–3.35], normoaeration 69.7 [44.6–82.2], hypoaeration 29.3 [13.6–49.4] and nonaeration (1.06% [0.37–6.02]). Next to the diaphragm, normoaeration dropped to $12 \pm 11\%$ and hypoaeration increased to $90 \pm 8\%$. No differences in aeration between groups were found at end-inspiration. Airway driving pressure (cm H₂O) was higher ($p = 0.002$) during VTc (9.8 ± 0.7) compared with VTi (7.6 ± 0.4). Lung strain was higher ($p = 0.014$) during VTc ($55 \pm 21\%$) than VTi ($38 \pm 10\%$). The stress index was higher ($p = 0.012$) during VTc (SI = 1.07 [0.14]) compared with VTi (SI = 0.93 [0.18]). This study indicates that body fat percentage influences the magnitude of lung, chest wall, and total respiratory system elastance and resistance, as well as functional residual capacity. Further, these results indicate that obese dogs have extensive areas

of hypo-aerated lungs, especially in caudodorsal regions. Finally, lung strain and airway driving pressure, surrogates of lung deformation, are higher during VTc than during VTi, suggesting that in obese anesthetized dogs, ventilation protocols based on IBW may be advantageous.

Keywords: obese, dogs, mechanical ventilation, ideal body weight, current body weight, anesthesia

INTRODUCTION

Overweight and obesity, defined as the excessive accumulation of adipose tissue, is becoming more common in veterinary patients, with studies reporting the prevalence of combined overweight and obesity as high as 45% (1).

In people, increased deposits of abdominal and intrathoracic fat result in significant alterations in respiratory mechanics, lung volumes, and gas exchange (2). In humans undergoing general anesthesia, functional residual capacity (FRC) decreases exponentially as body mass index increases (2). Although a decrease in FRC is also described for lean anesthetized people, the increased abdominal content and intraabdominal pressure result in increased loads on certain lung regions in the obese. Increased respiratory system elastance—the reciprocal of compliance-, impaired gas exchange and increased respiratory system resistance (R_{aw}) usually accompany the reductions in FRC. Therefore, mechanical ventilation in obese human patients is challenging, and requires careful planning to prevent the development of postoperative pulmonary complications (3). For instance, tidal volume (VT) in obese human patients undergoing mechanical ventilation is calculated based on predicted, instead of current, body weight (3). In obese mice, mechanical ventilation using VT based on current body weight results in altered lung mechanics and associated lung inflammation, when compared with ventilation using ideal body weight (IBW) (4).

Obese dogs share many similarities with obese people (5). For instance, it has been shown that awake obese dogs have reduced FRC and VT and increased respiratory rates (6–8). Sedated obese dogs have been shown to have impaired oxygenation (7). There is, however, very little information regarding the respiratory mechanics and lung aeration in obese dogs undergoing general anesthesia and mechanical ventilation, and most of the available information is extrapolated from obese people and experimental research. Moreover, it is unknown whether in obese dogs, VT should be calculated based on ideal vs. current body weight.

In the present study, we aimed at characterizing the respiratory system mechanics, gas exchange, and lung aeration in a small cohort of anesthetized and mechanically ventilated obese dogs. Moreover, we aimed at comparing the effects of using a VT calculated based on current vs. ideal body weight. We hypothesized that this population of obese dogs would have large areas of hypo or non-aerated lung tissue, especially in the caudodorsal regions, and that a ventilation protocol using VT based on ideal, as compared to current body weight, would result in decreased airway pressures and improved lung aeration.

MATERIALS AND METHODS

This study was approved by the Ethical Committee for Clinical Study in Animal Patients of the Department of Emergency and Organ Transplantation, University of Bari, Italy (Protocol 11/2017).

Animals

This was a prospective, randomized, controlled clinical trial that included client-owned dogs presented to the Veterinary Hospital at the University of Bari. For each case, a written consent form was signed by the dog owners, in compliance with the Italian Welfare Act and Statutes of the University of Bari. The study population consisted of dogs of different breeds referred to the Section of Veterinary Clinics and Animal Production of the Department of Emergency and Organ Transplantation (DEOT). All dogs were affected by abdominal or mammary gland tumors and were scheduled for a thoracic CT scan to evaluate for the presence of pulmonary metastasis. All patients underwent a complete physical examination and a standard radiographic examination of the thorax before induction of general anesthesia. Body condition score (BCS) was assessed based on a 9 point validated scale considering clinical inspection and body palpation (9). Although, there is not an established criterion in veterinary medicine, for the purpose of this study, only dogs with a BCS of ≥ 8 out of 9 were considered obese and were included in the study (10). Therefore, the inclusion criteria for the study was a BCS ≥ 8 out of 9, a normal chest radiograph and the absence of cardiac disease at a stage \geq than B2, based on the ACVIM classification. Dogs in which pulmonary metastasis or other major lung pathologies were detected in the CT scans were excluded from the study. Abnormal blood tests results were not considered as criteria for exclusion from the study.

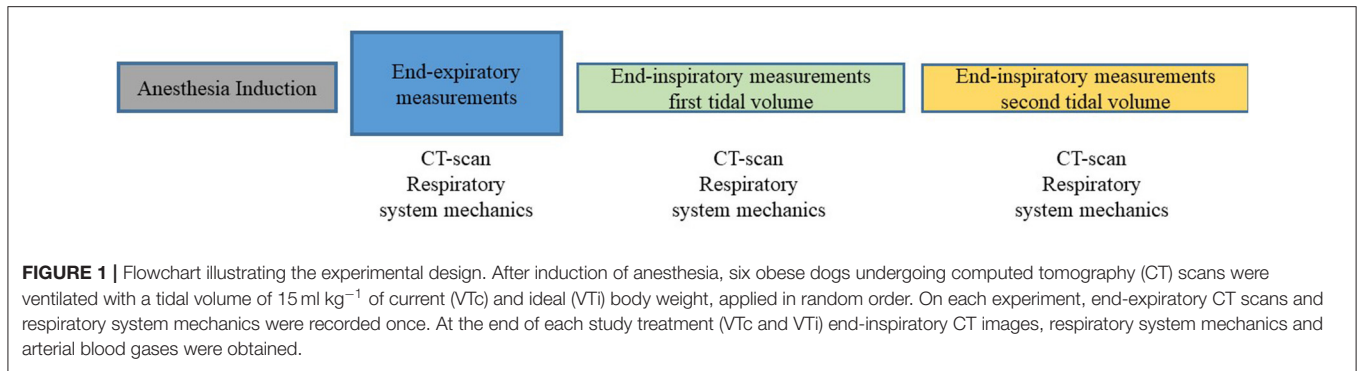
Dogs were also classified as barrel-chested, deep-chested or intermediate-chested (11).

Estimation of Ideal Body Weight

Current body weight was determined before the induction of anesthesia using an electronic scale. Ideal body weight was calculated from the current body weight based on the following formula:

$$\text{Ideal body weight (kg)} = \text{current body weight} - [\text{body fat (\%)} \times \text{current body weight}]$$

Where body fat (%) corresponds to the percentage of body fat computed based on the following morphometric gender specific



formulas (12):

$$\begin{aligned} \text{Males (\% body fat)} &= -1.4 (\text{HS cm}) + 0.77 (\text{PC cm}) + 4 \\ \text{Females (\% body fat)} &= -1.7 (\text{HS cm}) + 0.93 (\text{PC cm}) + 5 \end{aligned}$$

Where HS correspond to the length (in cm) from tuber calcaneus to midpatellar ligament (i.e., hock-to-stifle length) and PC to the pelvic circumference measured around the level of the flank.

Anesthesia and Monitoring

All dogs were sedated with acepromazine (Prequillan 1%, Fatro Spa, 20 µg kg⁻¹) intramuscularly (IM) followed 20 min later with IM morphine (Morfina Cloridrato 1%, Molteni Spa, 0.3 mg kg⁻¹). General anesthesia was induced with intravenous propofol titrated to effect (Proposure 1%, Merial Spa, 5–7 mg kg⁻¹). After orotracheal intubation with a cuffed endotracheal tube (Teleflex Medical Srl, Italy), dogs were positioned in dorsal recumbency and anesthesia was maintained with isoflurane (IsoFlo, Virbac Spa, Italy) in oxygen. Dogs were then connected to a mechanical ventilator (Siemens Servo 900C, Siemens Elma) equipped with a dedicated vaporizer (Siemens 950, Siemens Elma) and a standard nonrebreathing circuit (Flextube; Intersurgical Ltd, Italy). Dogs were ventilated in the volume-controlled mode with a VT adjusted according to the study protocol (see below), inspiratory to expiratory time ratio 1:2, an inspiratory pause 25% of the inspiratory time and the respiratory rate adjusted to maintain the end-tidal partial pressure of carbon dioxide between 35 and 45 mmHg. The end-tidal concentration of isoflurane was maintained between 1.3 and 1.5%. A lactated Ringer solution was infused at 5 ml kg h⁻¹ during anesthesia. Pulse oximetry, heart rate and rhythm, esophageal temperature, end-tidal CO₂ and noninvasive arterial blood pressure were continuously monitored with a multiparameter monitor (SC 6002XL, Siemens, MA).

Study Protocol

During volume-controlled ventilation, dogs were ventilated with a VT of 15 ml kg⁻¹ based on the current or IBW. Each dog received, in the same anesthetic episode, 20 min of ventilation with VT based on the IBW (VTi) and 20 min of ventilation based on the current body weight (VTc). The sequence of the treatments was assigned based on a simple randomization protocol, which relied on a predetermined table. The sequence of the treatments was based on a simple randomization

protocol (MedCalc Software version 19.7.4, Belgium) which established the assignment of each dog to group A or group B. Group A received first the VTi and then the VTc ventilation protocol. The sequence of the events in the Group B was the reversed. On each experiment, end-expiratory CT images of the thorax and respiratory system mechanics were obtained once, 15 min after anesthesia induction. At the end of each study treatment (VTc and VTi) end-inspiratory CT images of the thorax, respiratory system mechanics and arterial blood gases were obtained. Therefore, for each dog, we report 1 set of baseline end-expiratory images and 2 sets of end-inspiratory images, respiratory mechanics, and arterial blood gases (see **Figure 1**). Arterial blood samples were collected before measurements of respiratory mechanics and lung aeration and analyzed immediately (Idexx VetStat, Idexx Laboratories Inc., ME). Measured blood gases were corrected for the esophageal temperature of the dog (maintained between 37 and 38.5°C throughout the procedure) at the time of sample collection. Computed tomography images were obtained during muscle relaxation, achieved with an intravenous bolus (0.4 mg kg⁻¹) of rocuronium (Rocuronium Kabi 10 mg mL⁻¹, Italy). At the end of the study, the train-of-four (TOF) ratio was measured over the peroneal nerve (TOF-Watch, Organon, Dublin, Ireland) and a dose of neostigmine (0.02 mg kg⁻¹, Intrastigmina, Italy) was given immediately after a dose of atropine (0.02 mg/kg, Atropina Solfato, Ati Srl, Italy) if the TOF activity was < 0.9 (13). Dogs were discharged from the hospital at the end of the day.

The oxygen content-based index F-shunt was calculated using validated formulas (14).

CT Scan

Lung Volumes and Aeration Distribution

The methodology for CT scanning and calculation of lung aeration has been described elsewhere (15). Briefly, full thoracic CT scans were performed (GE ProSpeed sx, General Electric, New York, NY). End-expiratory images were obtained 15 min after anesthesia induction at an airway pressure (P_{aw}) of zero cmH₂O, by disconnecting the patient from the circuit and clamping the endotracheal tube. End-inspiratory images were taken at the end of a 4-s inspiratory pause. Pressure was maintained constant inside the lung by clamping the endotracheal tube during the pauses. The clamp was

then released and baseline ventilator settings resumed. End-inspiratory images were obtained at the end of a 20-min period of ventilation with both VTc and VTi.

CT images were obtained at 120 kVp and 160 mA; the matrix size was 512×512 , field of view 35 cm, and pitch 1.5. Images were reconstructed with 10 mm slice thickness and analyzed with the VELAS software[®] (Veterinary version of Maluna[®] by P. Herrmann, University of Göttingen Germany). Both right and left lungs were analyzed. The outer boundary of the lung was traced along the inner aspect of the ribs and the inner boundary along the mediastinal organs. Areas of the hilum containing the trachea, main bronchi, and vessels were excluded. Functional residual capacity (mL) and end-inspiratory lung volumes (EILV, mL) were computed by including pixels with densities between -1.000 and 100 HUs (CT number) during the end-expiratory and end-inspiratory pauses, respectively. Volumes were calculated according to the following formula:

$$\text{Gas volume (mL)} = \text{CT number}/(-1.000) \times \text{voxel volume}$$

Where each voxel is a pixel with a square base of 0.59 mm on each side and a height corresponding to the CT slice thickness (10 mm). For each dog, the data acquired in each CT image were then added together to yield the total lung volumes at end-expiration and end-inspiration. Lung strain was calculated as:

$$\text{Global lung strain (\%)} = [(EILV - FRC)/FRC] \times 100$$

For the analysis of global lung aeration, lung tissue was classified according to its gas/tissue content as hyperaerated ($-1,000$ to -901 HUs), normally aerated (-900 to -501 HUs), hypoaerated (-500 to -101 HUs), or nonaerated (-100 to 100 HUs) (15). To evaluate differences in aeration in the ventrodorsal direction, the software semi-automatically divided the lung into three equal regions of interest (ventral, intermediate, and dorsal). Aeration was also evaluated in the craniocaudal direction by plotting the calculated aeration for each axial slide.

In addition, the end-expiratory CT scan of an obese dog from this study and an end-expiratory CT scan from a lean dog of an unrelated, ongoing study, were used to create a 3D reconstruction of the lungs showing only the hypoaerated tissue. The DICOM data of each dog was imported into specialized segmentation software (Mimics Research, version 21, Leuven, Belgium) and thresholding masks were applied to segments of hypoaerated lung tissue. The mask for this lung category was manually split to remove any regions outside of the lung which may have been included based on the threshold values. The resulting models were exported in STL format, converted to OBJ format, combined into a single file using Blender (www.blender.org) and uploaded to Sketchfab (www.sketchfab.com) for display. A MP4 video was created from the Sketchfab model using the screen capture feature in PowerPoint (Microsoft, USA).

Regional Volumetric Lung Strain in One Dog

Regional volumetric strain in the lung parenchyma of one dog was determined from CT lung images following the

biomechanical analysis method developed by Hurtado et al. (16, 17). A strain analysis was performed based on a tetrahedral mesh of the lung reconstructed from a segmentation of the end-expiratory image. To report the results, regions of interest (ROIs) were defined by grouping sets of neighboring elements of the lung mesh so that ROIs divided the domain along the craniocaudal and ventrodorsal directions in roughly equal volume compartments. Both directions were intersected to allow for a two-dimensional spatial analysis of the quantities of interest. These directions, when intersected, gave a matrix of 5×5 ROIs, each with independent information on regional volumetric strain. Where the craniocaudal and dorsoventral segments did not intersect, that region was void. This technique is currently very time consuming and expensive, explaining the reason to include only one dog that best represented the average observed results.

Respiratory System Mechanics

The methodology for evaluation of respiratory mechanics has been described elsewhere (15). Briefly, gas flow was measured with a calibrated heated pneumotachograph (Fleisch No. 2, Fleisch, Switzerland) connected to a calibrated differential pressure transducer (Diff-Cap, Special Instruments GmbH, Germany). Prior to each experiment, it was verified that the pneumotachogram was linear over the range of gas flows. Tidal volume was obtained by integration of the flow signal. The P_{aw} (mmHg) was measured proximal to the endotracheal tube.

A 5-Fr balloon-tipped catheter system (Cooper Surgical[®], USA) was used to measure esophageal pressure, as an estimate of pleural pressure. An esophageal balloon (volume, 10 mL) was introduced through the dog's mouth and advanced within the distal third of the esophagus. The catheter then connected to a pressure transducer. The balloon was then filled with ~ 1 mL of air, following the description by Mauri et al. (18). Briefly, the most adequate filling volume of the balloon was determined by progressively inflating the balloon, within the catheter specific range of filling volumes, finally selecting the lowest volume associated with the largest tidal swings. Finally, correct catheter position was confirmed by observation of cardiac oscillations and by performance of the positive pressure occlusion technique (18). Variables were displayed and collected for posterior analysis through a 12-bit analog-to-digital converter board (DAQCard 700; National Instruments, TX, USA) at a sampling rate of 200 Hz (ICU Lab, KleisTEK Engineering, Italy).

The static mechanical properties were determined by applying 4-s end-inspiratory and end-expiratory airway occlusions at the time of end-inspiratory and end-expiratory CT imaging, respectively (19). Total end-expiratory pressure of the respiratory system ($PEEP_{RS}$) and of the chest wall ($PEEP_{CW}$) were measured as the plateau pressure in P_{aw} and P_{ES} , respectively, at the end of the expiratory pause.

The airway driving pressure (ΔP_{awO}) and the tidal variation in esophageal pressure (ΔP_{ES}) (20) were calculated as:

$$\Delta P_{awO} = P_{plat} - PEEP_{RS}$$

$$\Delta P_{ES} = P_{ESplat} - PEEP_{CW}$$

Where P_{plat} is the plateau pressure measured at the end of the 4-s inspiratory pause. Thereafter, the transpulmonary driving pressure (ΔP_L) was calculated as:

$$\Delta P_L = \Delta P_{\text{awO}} - \Delta P_{\text{ES}}$$

Since in humans obesity has been shown to induce negative end-expiratory P_L , this variable was also calculated as:

$$\text{End - expiratory } P_L = \text{PEEP}_{\text{RS}} - \text{PEEP}_{\text{CW}}$$

The elastance of the respiratory system (E_{RS}), lung (E_L), and chest wall (E_{CW}) were calculated as:

$$E_{\text{RS}} (\text{cmH}_2\text{O mL}^{-1}) = \Delta P_{\text{awO}} / \text{VT}$$

$$E_L (\text{cmH}_2\text{O mL}^{-1}) = \Delta P_L / \text{VT}$$

$$E_{\text{CW}} (\text{cmH}_2\text{O mL}^{-1}) = \Delta P_{\text{ES}} / \text{VT}$$

Respiratory system resistance (R_{aw}) was calculated as (21):

$$R_{\text{aw}} (\text{cmH}_2\text{O L sec}^{-1}) = (P_{\text{peak}} - P_{\text{plat}}) / \text{inspiratory flow}$$

Where P_{peak} is the airway pressure measured immediately prior to the end-inspiratory pause. Elastance values are reported indexed by kg of IBW. Resistance values are reported indexed by kg of $\text{IBW}^{-0.891}$ (22).

The stress index (SI) was estimated using a validated approach based on the Levenberg-Marquardt method (23). Briefly, during constant flow inflation, the dynamic pressure-time curve can be described by a power equation:

$$P_{\text{aw}}(t) = a \times t^b + c$$

Where t is time and a , b and c are constant coefficients. The coefficient b (SI) is a dimensionless number that describes the shape of the pressure-time curve. When $b < 1$, the pressure-time curve presents a downward concavity, indicating that elastance decreases with time during the breath. When $b > 1$, the pressure-time curve presents an upward concavity, indicating that intratidal elastance increases with time. When $b = 1$, the pressure-time curve is straight, indicating that elastance is constant over time. In the present study, an $\text{SI} < 0.95$ is defined as tidal recruitment/derecruitment (RD) and an $\text{SI} > 1.05$ is defined as tidal overdistension, whereas a straight line ($0.95 > \text{SI} < 1.05$) is defined as a constant elastance (24). An example obtained from the analysis of one dog is shown in **Supplementary Figure 1**. This evaluation was performed with an automated software (ICU Lab, KleisTEK Engineering, Italy).

Statistical Analysis

The Shapiro-Wilk test was used to test data for normality. Data are reported as mean \pm SD or median [range] where appropriate. Differences in respiratory mechanics, arterial blood gases and CT scan variables between treatments were evaluated with linear mixed models (for normally distributed data) and with generalized linear mixed models (for non-normally distributed data) with time, treatment, and the interaction between time and

treatment as fixed effects, and dog ID and the interaction between dog ID and treatment as random effects. Differences in aeration at end-expiration between regions in the ventrodorsal direction were compared with two-way ANOVA followed by Tukey test for multiple comparisons. Simple linear regression was used to evaluate the association between: (a) body fat percentage and E_{RS} , E_L , and E_{CW} ; (b) body fat percentage and lung aeration at end-expiration; (c) body fat percentage and FRC indexed by kg of IBW (FRC kg^{-1} IBW); and (d) body fat percentage and R_{aw} indexed by kg of $\text{IBW}^{-0.891}$, and the coefficients of determination (R^2) reported. Due to the uneven distribution of the nominal categorical variable “body conformations” and the small number of dogs included, no analysis was performed on the association of this variable with the evaluated outcomes. A $p < 0.05$ was considered significant. All statistical analyses were performed using JMP Pro 14 (SAS, USA) and GraphPad Prism 8 (GraphPad Software, USA).

RESULTS

Patient Characteristics and Gas Exchange

Six adult (2–9 years of age) dogs (1 male, 5 female) with a body condition score between 8 and 9 and a percentage of body fat between 20 and 43% were included in the study (**Table 1**). The arterial partial pressure of O_2 (PaO_2 , mmHg) was not different ($p = 0.977$) between treatments [536 (232–584) and 514 (280–533) during VTc and VTi, respectively]. No differences were found ($p = 0.999$) in the F-shunt index (%) between VTc (11.5 ± 8.7) and VTi (11.3 ± 6.6) or in the PaCO_2 (mmHg) (38.8 ± 5.7 and 43.8 ± 8.8 during VTc and VTi, respectively).

CT Scan

End-Expiration

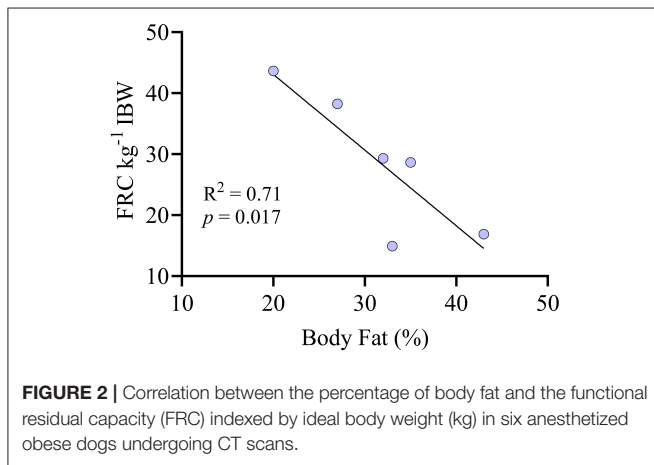
The FRC was $28.6 \pm 11.4 \text{ mL kg}^{-1}$ of IBW. There was a significant negative correlation between FRC kg^{-1} IBW and the percentage of body fat (**Figure 2**). In whole lung evaluation, percentages of lung volume with hyperaeration (0.03% [0.00–3.35]) and nonaeration (1.06% [0.37–6.02]) were very low (**Figure 3A**). The percentage of normally aerated and hypoaerated lung volume was 69.7% [44.6–82.2] and 29.3 [13.6–49.4], respectively (**Figure 3A**). There was a significant ($p = 0.014$) positive correlation between percentage of hypoaeration and body fat percentage ($R^2 = 0.82$). The percentage of normoaeration showed a nonsignificant ($p = 0.051$) negative correlation ($R^2 = 0.65$) and the percentage of nonaeration showed a nonsignificant ($p = 0.099$) positive correlation ($R^2 = 0.53$) with body fat percentage.

In the ventrodorsal direction, the percentage of hypoaerated tissue was higher ($p < 0.001$) and the percentage of normally aerated tissue was lower ($p < 0.001$) in the dorsal region compared with the ventral and intermediate regions (**Figure 3B**). **Figure 4** shows that in the craniocaudal direction, most of the midcranial lung tissue was normoaerated ($\sim 75\%$), with the remaining being mostly hypoaerated. In the most caudal slices, the percentage of normoaeration decreased and that of hypoaeration increased, reaching 90% of lung tissue in the slice closest to the diaphragm (see **Figure 4**).

TABLE 1 | Patient characteristics in a group of six anesthetized obese dogs with varying degrees of body fat percentage undergoing computed tomography scans, and ventilated with tidal volumes based on current vs. ideal body weight.

Cases	Sex	Age (months)	Current weight (kg)	Ideal weight (kg)	Body fat percentage (%)	BCS (1–9)	Breed	Chest conformation
1	M	48	45	40.4	20	9	Corso	Deep
2	F	60	15	10.2	33	9	Mixed	Intermediate
3	F	24	12	8.7	27	9	Mixed	Barrel
4	F	72	19	13	32	8	Mixed	Intermediate
5	F	108	17	10	43	9	Mixed	Intermediate
6	F	60	19	12	35	9	Mixed	Deep

BCS, body condition score; F, female; M, male.



Supplementary Videos 1, 2 show the distribution of hypoerated lung tissue in the reconstructed lungs of a lean (from an ongoing, unpublished study) and an obese dog (from the present study), respectively.

End-Inspiration

In whole-lung evaluation at end-inspiration, normoerated tissue increased ($p = 0.024$) and hypoerated tissue decreased ($p = 0.027$) compared to end-expiration, with both tidal volumes (**Figure 5A**). There were no differences in aeration between treatments in whole-lung evaluation.

In the ventrodorsal direction during VTc, normally aerated tissue increased ($p = 0.005$) whereas hypoerated ($p = 0.007$) and nonaerated tissue decreased ($p < 0.032$) only in the dorsal region compared with the end-expiratory images (**Figure 5B**). There were no differences between end-expiration and end-inspiration during VTi in any of the regions (**Figure 5C**). No regional differences were seen between VTc and VTi at end-inspiration.

Volumetric Lung Strain

As shown in **Figure 6A**, global lung strain was significantly ($p = 0.014$) higher with VTc compared with VTi. In the individual dog in which regional volumetric strains were calculated, the global volumetric strain during VTc was 54%, whereas during VTi was 34%. However, regional volumetric strains ranged from 14 to

181% during VTc and from 2 to 123% during VTi (**Figure 6B**). Regional strains were higher during VTc in 20 of 23 regions evaluated in this dog.

Respiratory System Mechanics

Respiratory mechanics are shown in **Table 2**. Global mechanics were obtained in all dogs, whereas partitioned mechanics were not properly obtained in two animals, therefore these results are based on four dogs only. Tidal volume was higher ($p = 0.045$) during VTc compared with VTi. Tidal volume indexed by current body weight (mL kg^{-1}) was higher ($p < 0.001$) during VTc than during VTi. Peak airway pressure, P_{plat} , P_{ESplat} , and ΔP_{awO} were significantly higher during VTc compared with VTi ($p < 0.05$). Other variables were not different between treatments. End-expiratory P_{TP} was negative. Respiratory system resistance indexed by $\text{IBW}^{-0.891}$ showed a positive correlation with body fat percentage ($R^2 = 0.75$, $p = 0.024$).

The percentage of body fat showed a positive correlation with E_{RS} , E_{L} , and E_{CW} , as shown in **Figure 7**. The SI (**Figure 8**) was higher ($p = 0.012$) during VTc (SI = 1.07 [0.14]) compared with VTi (SI = 0.93 [0.18]).

DISCUSSION

This study represents an initial characterization of partitioned respiratory system mechanics and thoracic CT findings in obese dogs undergoing general anesthesia and mechanical ventilation with VT based on ideal vs. current body weight. The results of the present work can be summarized as follows. First, in this small cohort of obese adult dogs, there is a high percentage of hypoerated tissue, especially in the most dependent areas and those close to the diaphragm. Interestingly, the percentage of hypoerated tissue increases linearly with the percentage of body fat. Second, global lung strain and ΔP_{awO} are significantly higher during VTc, whereas global lung strain with VTi is similar to that described for lean dogs (19), suggesting a more physiologic tidal inflation during the latter. Third, although P_{plat} is higher during VTc, elastances are not significantly different compared with VTi. Likewise, R_{aw} , indexed by an allometric coefficient, is comparable between treatments. Both the elastances and the R_{aw} are significantly correlated with body fat percentage. Finally, SI, a variable defining the shape of the pressure-time curve during

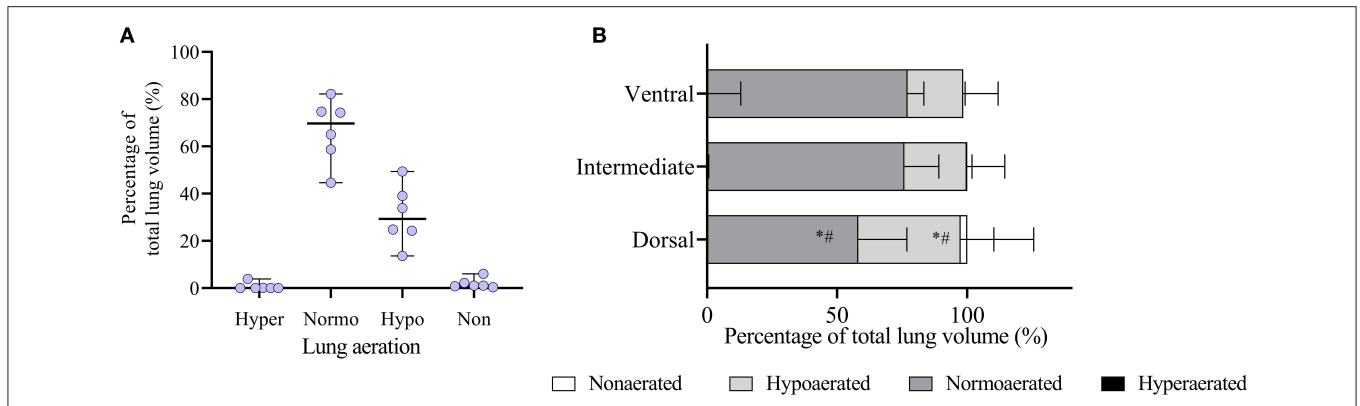


FIGURE 3 | Analysis of lung aeration data obtained by computed tomography (CT) scans during an end-expiratory pause in six obese dogs undergoing anesthesia. **(A)** Whole lung aeration analysis. Hyper, hyperaerated; Normo, normoerated; Hypo, hypoerated; Non, nonaerated. **(B)** Regional analysis of aeration in the ventrodorsal direction is shown. Since dogs were in dorsal recumbency, the ventral region represents the nondependent lung and the dorsal region represents the dependent lung. * $p < 0.05$ compared to normoeration in the ventral and intermediate regions; # $p < 0.05$ compared to hypoeration in the ventral and intermediate regions.

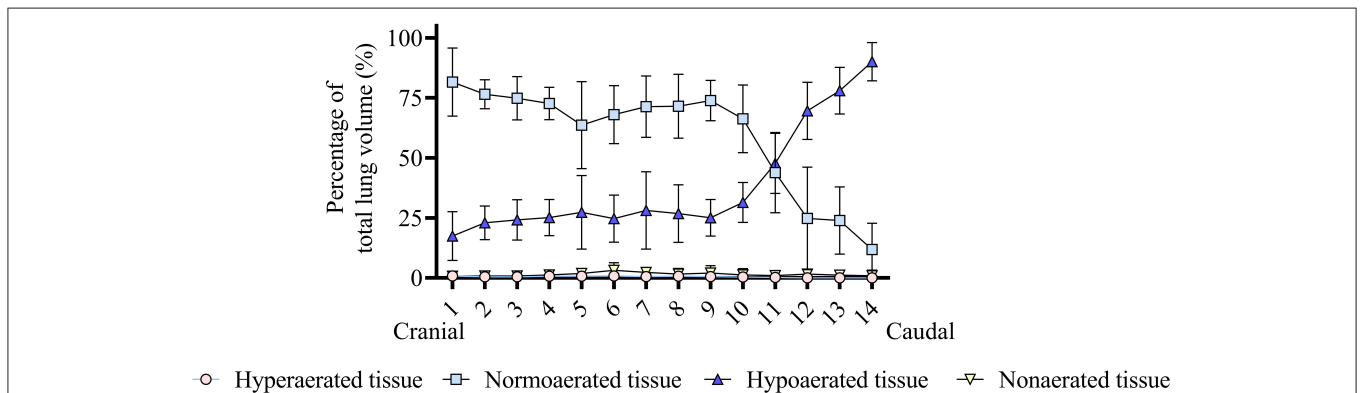


FIGURE 4 | Analysis of the craniocaudal distribution of lung aeration in six obese dogs undergoing anesthesia. It can be seen that most of the midcranial lung tissue is normoerated, whereas hypoeration becomes predominant in the caudal lung. Hyperaerated tissue and nonaerated tissue are scarce.

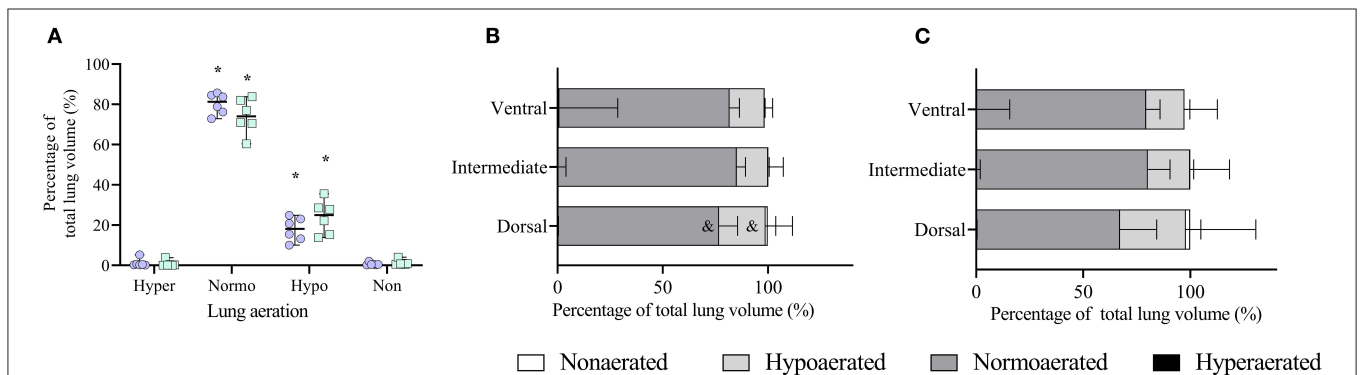


FIGURE 5 | Analysis of lung aeration data obtained by computed tomography (CT) scans during an end-inspiratory pause in six obese dogs undergoing anesthesia. **(A)** Whole end-inspiratory aeration is shown during ventilation with tidal volumes based on current (VtC, open circles) and ideal (VtI, open squares) body weight. Hyper, hyperaerated; Normo, normoerated; Hypo, hypoerated; Non, nonaerated. * $p < 0.05$ compared to the respective aeration during end-expiration (**Figure 4A**). **(B)** Regional end-inspiratory aeration during treatment VtC. & $p < 0.05$ compared to the respective aeration within the same region during end-expiration (**Figure 3B**). **(C)** Regional end-inspiratory aeration during treatment VtI.

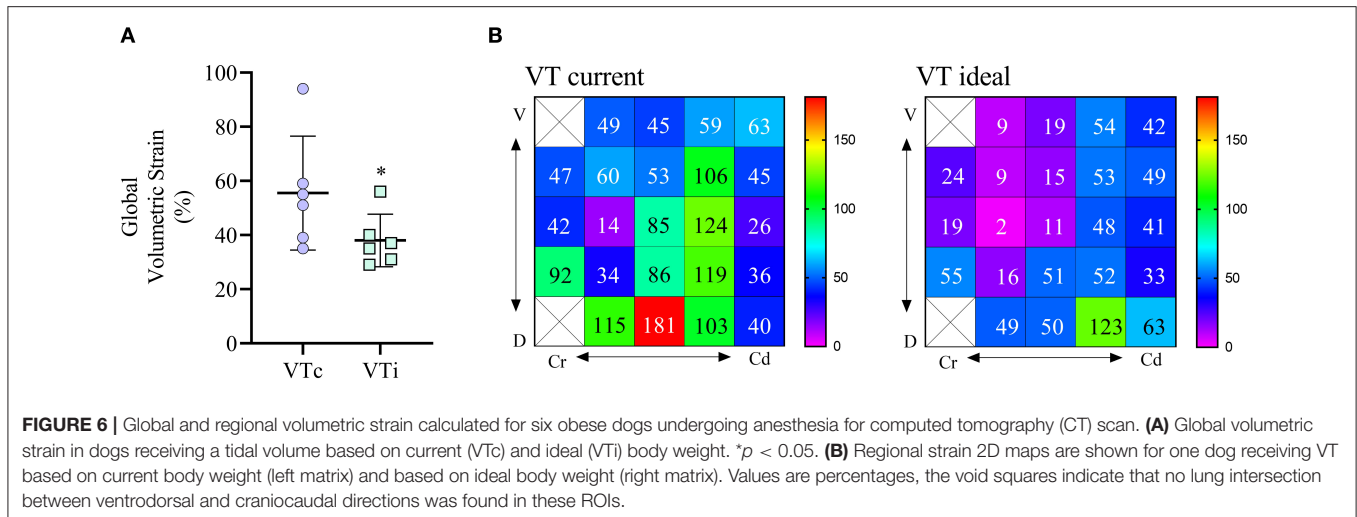


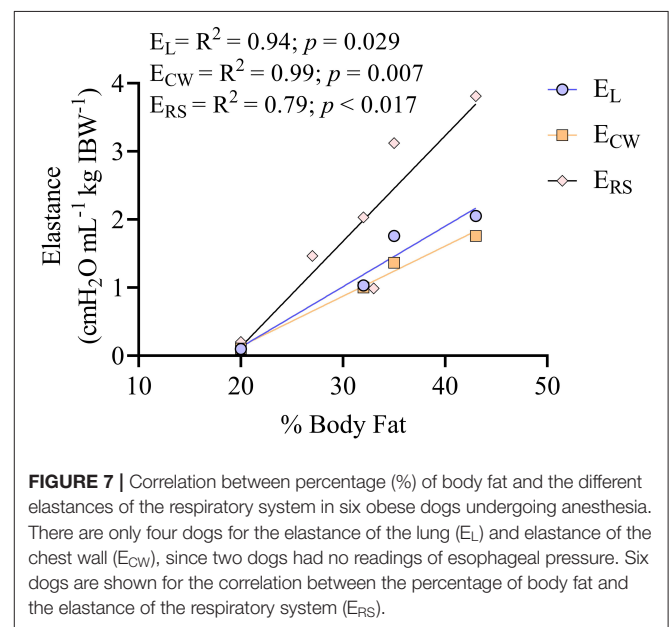
TABLE 2 | Global and partitioned respiratory system mechanics in a group of six obese anesthetized dogs undergoing computed tomography scans, and ventilated with tidal volumes based on current vs. ideal body weight.

Variable	V _T current	V _T ideal	p-value
VT (mL)	323 ± 75	240 ± 73	<0.001
VT kg ⁻¹ current (mL kg ⁻¹)	15.2 ± 0.2	10.7 ± 0.6	0.001
P _{peak} (cmH ₂ O)	15.9 ± 1.3	12.2 ± 1	<0.001
P _{plat} (cmH ₂ O)	10.2 ± 0.6	7.9 ± 0.4	0.046
PEEP _{RS} (cmH ₂ O)	0.3 ± 0.1	0.3 ± 0.1	0.947
P _{ESplat} (cmH ₂ O)	6.8 ± 0.5	6.2 ± 0.4	0.046
PEEP _{CW} (cmH ₂ O)	2.7 ± 0.9	2.7 ± 0.9	0.671
ΔP _{awO} (cmH ₂ O)	9.8 ± 0.7	7.6 ± 0.4	0.002
ΔP _{ES} (cmH ₂ O)	3.9 ± 0.3	3.4 ± 0.2	0.061
ΔP _L (cmH ₂ O)	6.0 ± 1.1	4.1 ± 0.5	0.062
E _{RS} IBW ⁻¹ (cmH ₂ O L ⁻¹ kg ⁻¹)	2.6 ± 1.6	2.3 ± 1.5	0.309
E _L IBW ⁻¹ (cmH ₂ O L ⁻¹ kg ⁻¹)	1.5 ± 1.2	1.2 ± 0.9	0.394
E _{CW} IBW ⁻¹ (cmH ₂ O L ⁻¹ kg ⁻¹)	1.0 ± 0.7	1.1 ± 0.7	0.461
E _L /E _{RS}	0.56 ± 0.06	0.52 ± 0.04	0.062
EE P _L (cmH ₂ O mL ⁻¹)	-2.3 ± 0.9	-2.3 ± 0.9	>0.999
R _{aw} (cmH ₂ O L s ⁻¹ kg IBW ^{-0.819})	2.2 ± 1.6	1.6 ± 1.3	0.157
Respiratory rate (per min)	14 ± 6	22 ± 7	0.130

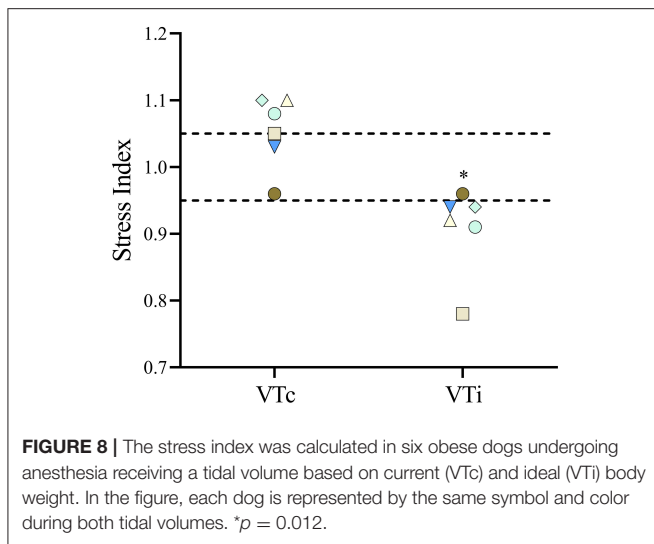
VT, tidal volume; VT kg⁻¹ current, tidal volume by current body weight; VT kg⁻¹ ideal, tidal volume by ideal body weight; P_{peak}, peak airway pressure; P_{plat}, plateau airway pressure; PEEP_{RS}, positive end-expiratory pressure of the respiratory system; P_{ESplat}, plateau of the esophageal pressure; PEEP_{CW}, positive end-expiratory pressure of the chest wall; ΔP_{awO}, driving airway pressure; ΔP_{ES}, driving esophageal pressure; ΔP_L, driving transpulmonary pressure; E_{RS} elastance of the respiratory system; E_L elastance of the lung; E_{CW}, elastance of the chest wall; E_L/E_{RS}, ratio of the elastance of the lung to the elastance of the respiratory system; EE P_L, end-expiratory transpulmonary pressure; R_{aw} respiratory system resistance indexed by ideal body weight^{-0.819}. Variables requiring the value of esophageal pressure for its calculation (P_{ESplat}, PEEP_{CW}, ΔP_{ES}, ΔP_L, E_L, E_{CW}, E_L/E_{RS}, and EE P_L) were obtained from four dogs. All other variables were calculated from six dogs.

constant flow, suggests tidal overdistension during VTc and tidal RD during VTi.

The prevalence of overweight and obesity in dogs is increasing and some studies report that when included together, up to



45% of the overall dog population may fall into this category (1, 5). Besides inducing changes in several other systems, obesity can significantly alter the normal function of the respiratory system (5). In humans, the accumulation of adipose tissue in the abdomen results in compression of the thorax with ensuing reductions in FRC (2). In the present study, the different elastances normalized to IBW were higher than those previously reported in populations of lean adult anesthetized dogs (19, 25). In ventilated human patients, obesity is associated with increased E_{RS}, explained mostly by an increase in the E_L, and to a lesser extent by the E_{CW}. Lung collapse, with reductions in FRC, seem to be responsible for increases in E_L and E_{RS} (2, 26). Obese dogs had a large proportion of hypo-aerated lung tissue, which is probably responsible for the increased E_L and E_{RS} seen in this study. Further studies should evaluate



whether these differences are still apparent when comparing respiratory mechanics of lean and obese dogs with similar body conformations. Interestingly, our study also showed a strong correlation between the normalized elastances and the body fat percentage, suggesting that overweight and obesity in anesthetized dogs can lead to significant alterations in respiratory system elastance.

A common finding in obese people is an increased R_{aw} , most likely due to reductions in lung volumes (2, 26, 27). Although atelectasis in the present study was very low, as evidenced by the minimal amount of nonaerated lung tissue, hypoaeration was significant and the FRC kg^{-1} IBW was lower compared with a population of lean dogs previously reported by our group (mean FRC $\text{kg}^{-1} = 37 \text{ mL kg}^{-1}$) (19). Moreover, we observed a significant negative correlation between FRC kg^{-1} IBW and body fat percentage that is worth exploring further. Decreased FRC has been ascribed as the main factor behind an increased R_{aw} in obese people. The extent of hypoaerated tissue in the lungs of the dogs in the present study, especially in the ventral and caudal areas, was large. In anesthetized human patients in supine position, most atelectasis has been reported to occur near the diaphragm, and less toward the apex, similar to our results (28). In lean healthy dogs under anesthesia, a similar pattern of distribution has been observed, although the magnitude of hypoaerated tissue is significantly less than that of this population of obese dogs (unpublished data). **Supplementary Videos 1, 2** show the 3D distribution of hypoaerated tissue in a lean dog from an unrelated ongoing study and an obese dog from the present study, evidencing significantly more hypoaerated tissue in the obese dog under similar anesthetic conditions and positioning. Interestingly, our results also showed a positive correlation between body fat percentage and $R_{aw} \text{ kg}^{-1} \text{ IBW}^{-0.891}$. Therefore, when taken together with the correlation observed between the elastance and body fat percentage, our results suggest that obesity in dogs may increase both the elastic and resistive work of breathing. This could represent a clinical problem,

especially for spontaneously breathing obese dogs under sedation or anesthesia.

Aggressive mechanical ventilation leading to excessive parenchymal deformation in people has been associated with a high incidence of postoperative pulmonary complications (29, 30). Therefore, the appropriate setting of intraoperative ventilatory variables seems to play an important role in protecting the lungs from ventilator-induced lung injury. Volumetric lung strain is a measure of cyclic lung deformation and has been found to be one of the main determinants of ventilator-induced lung injury (31–33). In the present study, global volumetric lung strains were significantly lower during VTi compared with VTc. In fact, strains during VTi were comparable to a cohort of lean dogs (19), suggesting that in obese dogs, a protocol using VTi is more physiologic than VTc. The evaluation of regional lung strains in one dog revealed a wide range of values, suggesting that the determination of lung strain using global estimations can over, and more importantly, under estimate local strain values in this population. This is relevant considering that, especially during ventilation with VTc, potentially injurious values of strain developed in some regions (31, 34). Further studies are required to confirm these preliminary findings. Airway driving pressure has been used as a surrogate of global lung strain (33). As expected, VTc generated significantly higher ΔP_{awO} compared with VTi. Other estimates of lung distension such as the ΔP_L and the E_L were not different between treatments; however, there was a trend to higher values during VTc, which in view of other significant differences, such as ΔP_{awO} and lung strain, suggest that these trends may become significant if the sample size is increased, although the latter remains speculative. Similarly, the mean SI during VTc was at the high-end of the normal range, with two dogs exceeding this cut-off point (24). Although higher SI values suggest the presence of intratidal overdistension, the percentage of hyperaerated tissue in the end-inspiratory images was very low, even during VTc. However, prolonged inspiratory breath holds applied during static end-inspiratory CT imaging of the thorax can lead to significant intratidal redistribution of lung volumes (35), which can render different information compared with a dynamic parameter such as the SI. Future studies should evaluate tidal hyperaeration in obese dogs using such techniques as dynamic CT. It has to be considered, however, that normal SI values for dogs have not been validated. More importantly, prospective studies in obese dogs should evaluate whether protocols using VTi result in lung protection compared to those using VTc. In obese mice, ventilation based on VTc as compared to VTi increases the expression of several pulmonary inflammatory markers (4).

To the authors' best knowledge, this is the first study to report the end-expiratory P_L in obese dogs. In people, increased abdominal load leads to the regional generation of positive pleural pressures, which in turn can lead to the generation of negative end-expiratory P_L , especially in the absence of externally applied PEEP (26). Therefore, some authors advocate titrating PEEP to achieve values of end-expiratory P_L that are slightly positive (e.g., +2 cmH_2O) (26). This negative end-expiratory

P_L values could in part explain the reduced FRC kg^{-1} and the large proportion of hypoerated tissue observed in this study. Given the well-described limitations of using absolute esophageal pressure values and calculations derived from it (e.g., end-expiratory transpulmonary pressure), these results should be interpreted cautiously (26, 36). Interestingly, during VTi, the mean SI was 0.93, suggesting that external PEEP in these dogs could have been beneficial to prevent tidal RD and to improve lung aeration (24). Together, these data suggest that PEEP should be titrated in these patients to avoid negative values of end-expiratory P_L and to increase lung volumes, regardless of how the VT is set, and to normalize indices of tidal RD such as low SI values during ventilatory protocols using VTi.

An unexpected finding in the present study was the absence of major oxygenation impairment. Obese human patients undergoing mechanical ventilation have significant gas exchange abnormalities, resulting in venous admixture and shunt, associated most likely with the development of extensive atelectasis (2). In obese sedated dogs, oxygenation was impaired and oxygen tension-based indices improved after weight loss, suggesting a similar effect of obesity on oxygenation as that reported for obese humans (7). The reason for the lack of significant oxygenation impairment in the present study is unclear, but it may be related to several factors. For instance, dogs in the present study, unlike sedated obese dogs reported by Mosing et al. (7), were undergoing mechanical ventilation, which could have resulted in improved overall gas exchange and resulted in better oxygenation. Also, an important difference between dogs of this study and that of the sedated dogs is that the percentage of body fat was significantly lower (mean body fat percentage was 30% in the present study vs. 45% in the sedated dogs) (7). Similarly, although in the dogs reported here there was a significant proportion of hypoerated lung tissue, especially in dependent and caudal areas of the lung, the amount of nonaerated tissue was very low, which could have resulted in scarce intrapulmonary shunt formation and instead, the development of a larger proportion of low ventilation-to-perfusion units. Although areas of low ventilation-to-perfusion ratios can significantly alter gas exchange, these units tend to respond to increased oxygen concentrations by increasing their end-capillary oxygen content (37). Although high fractions of oxygen may lead to absorption atelectasis in some situations (38), recent studies in anesthetized dogs have shown that the effect of this phenomenon on gas exchange may not be as relevant as previously thought in dogs (39, 40). However, further prospective studies should evaluate the effects of extreme obesity with higher percentages of body fat on oxygenation in dogs, as in these cases it is possible that the extent of nonaerated tissue and intrapulmonary shunt may be higher, as is described in morbidly obese people.

Our study has significant limitations. First, the number of animals included is small. This was due to the difficulty in recruiting obese dogs that required anesthesia and mechanical ventilation for diagnostic CT scans. This limitation is even more significant when considering the partitioned respiratory mechanics, as only four dogs had correct measurements of esophageal pressure. Moreover, we used absolute values of

esophageal pressure as a surrogate of pleural pressure. Although this approach is methodologically convenient, studies have shown that absolute esophageal pressure measurements may not accurately reflect pleural pressure values in all conditions or areas of the chest (36), although other studies show that, following proper calibration, absolute esophageal pressure measurements are a good estimate of dependent pleural pressures (41). Therefore, future studies in clinical dogs should focus on the impact of these situations in the estimation of pleural pressure. Second, we only focused on the effects of VT on the measured outcomes; however, an equally important consideration regarding the ideal ventilatory settings in these patients is the use of PEEP, especially considering the negative values of end-expiratory P_L observed in the present study. In fact, lung strain, an important outcome measured in this study, depends not only on the cyclic variation of tidal volume but also on the baseline end-expiratory volume (i.e., the FRC), largely dependent on PEEP (33). However, since we anticipated a low rate of patient recruitment, our decision to focus only in one variable was pragmatic, in an attempt to capture the effect of the VT *per se*. Another limitation is that we did not include obese dogs undergoing surgery, especially for abdominal procedures and laparoscopies. In these patients, there could be an additive negative effect between obesity and abdominal manipulation or insufflation on the respiratory system (26). We performed only a single end-expiratory evaluation of CT images and respiratory mechanics in each dog, which compounds to the fact that no standardization of lung volume history was performed. This may be an important limitation of the present study and should be kept in mind when interpreting the results. Although, time could have created differences in end-expiratory aeration and mechanics, a study showed that end-expiratory lung volume did not change when ventilating anesthetized dogs with a tidal volume of 8 or 15 mL kg^{-1} (15). Moreover, we decided to omit one end-expiratory measurement in an attempt to reduce experimental duration and to spare dogs from another set of CT images.

In conclusion, in mechanically ventilated obese dogs, as the percentage of body fat increases, FRC decreases while the percentage of pulmonary hypoeration, R_{aw} , E_{RS} , E_L , and E_{CW} increase. Although no difference in gas exchange was noted, mechanical ventilation of obese dogs using VTi generated more physiologic volumetric lung strains and lower ΔP_{awO} than VTc, suggesting that the VTi may be more appropriate than VTc for mechanical ventilation of this canine patient population. Future studies should evaluate the impact of mechanical ventilation with VTi on the clinical outcomes of anesthetized obese dogs.

DATA AVAILABILITY STATEMENT

The raw data supporting the conclusions of this article will be made available by the authors, without undue reservation.

ETHICS STATEMENT

The animal study was reviewed and approved by Ethical Committee for Clinical Study in Animal Patients of the

Department of Emergency and Organ Transplantation, University of Bari, Italy. Written informed consent was obtained from the owners for the participation of their animals in this study.

AUTHOR CONTRIBUTIONS

JA: interpreted the data, analyzed the respiratory mechanics and the CT scans, performed the statistics, and wrote the manuscript. LL, VM, MS, and AC: participated in study design and experimental procedure. SG and MM-F: interpreted the data and critically reviewed the manuscript. IP: analyzed the

CT scans and created the 3d reconstructions of the lungs. DH and AP: critically reviewed the manuscript and performed the biomechanical analysis of regional strain. FS: designed the study, performed experimental procedures, data analysis, and manuscript review. All authors contributed to the critical revision of the paper and approved the final manuscript.

SUPPLEMENTARY MATERIAL

The Supplementary Material for this article can be found online at: <https://www.frontiersin.org/articles/10.3389/fvets.2021.704863/full#supplementary-material>

REFERENCES

- McGreevy PD, Thomson PC, Pride C, Fawcett A, Grassi T, Jones B. Prevalence of obesity in dogs examined by Australian veterinary practices and the risk factors involved. *Vet Rec.* (2005) 156:695–702. doi: 10.1136/vr.156.22.695
- Pelosi P, Croci M, Ravagnan I, Tredici S, Pedoto A, Lissoni A, et al. The effects of body mass on lung volumes, respiratory mechanics, and gas exchange during general anesthesia. *Anesth Analg.* (1998) 87:654–60. doi: 10.1213/00000539-199809000-00031
- Imber DA, Pirrone M, Zhang C, Fisher DF, Kacmarek RM, Berra L. Respiratory management of perioperative obese patients. *Respir Care.* (2016) 61:1681–92. doi: 10.4187/respcare.04732
- Guivarch E, Voiriot G, Rouze A, Kerbrat S, Tran Van Nhieue J, Montravers P, et al. Pulmonary effects of adjusting tidal volume to actual or ideal body weight in ventilated obese mice. *Sci Rep.* (2018) 8:6439. doi: 10.1038/s41598-018-24615-5
- Love L, Cline MG. Perioperative physiology and pharmacology in the obese small animal patient. *Vet Anaesth Analg.* (2015) 42:119–32. doi: 10.1111/vaa.12219
- Bach JF, Rozanski EA, Bedenice D, Chan DL, Freeman LM, Lofgren JL, et al. Association of expiratory airway dysfunction with marked obesity in healthy adult dogs. *Am J Vet Res.* (2007) 68:670–5. doi: 10.2460/ajvr.68.6.670
- Mosing M, German AJ, Holden SL, MacFarlane P, Biourge V, Morris PJ, et al. Oxygenation and ventilation characteristics in obese sedated dogs before and after weight loss: a clinical trial. *Vet J.* (2013) 198:367–71. doi: 10.1016/j.tvjl.2013.08.008
- Manens J, Ricci R, Damoiseaux C, Gault S, Contiero B, Diez M, et al. Effect of body weight loss on cardiopulmonary function assessed by 6-minute walk test and arterial blood gas analysis in obese dogs. *J Vet Intern Med.* (2014) 28:371–8. doi: 10.1111/jvim.12260
- Chun JL, Bang HT, Ji SY, Jeong JY, Kim M, Kim B, et al. A simple method to evaluate body condition score to maintain the optimal body weight in dogs. *J Anim Sci Technol.* (2019) 61:366–70. doi: 10.5187/jast.2019.61.6.366
- Brooks D, Churchill J, Fein K, Linder D, Michel KE, Tudor K, et al. 2014 AAHA weight management guidelines for dogs and cats. *J Am Anim Hosp Assoc.* (2014) 50:1–11. doi: 10.5326/JAAHA-MS-6331
- Asorey I, Pellegrini L, Canfran S, Ortiz-Diez G, Aguado D. Factors affecting respiratory system compliance in anaesthetised mechanically ventilated healthy dogs: a retrospective study. *J Small Anim Pract.* (2020) 61:617–23. doi: 10.1111/jsap.13194
- Mawby DI, Bartges JW, d'Avignon A, Laflamme DP, Moyers TD, Cottrell T. Comparison of various methods for estimating body fat in dogs. *J Am Anim Hosp Assoc.* (2004) 40:109–14. doi: 10.5326/0400109
- Jones RS, Auer U, Mosing M. Reversal of neuromuscular block in companion animals. *Vet Anaesth Analg.* (2015) 42:455–71. doi: 10.1111/vaa.12272
- Araos JD, Larenza MP, Boston RC, De Monte V, De Marzo C, Grasso S, et al. Use of the oxygen content-based index, Fshunt, as an indicator of pulmonary venous admixture at various inspired oxygen fractions in anesthetized sheep. *Am J Vet Res.* (2012) 73:2013–20. doi: 10.2460/ajvr.73.12.2013
- De Monte V, Bufalari A, Grasso S, Ferrulli F, Crovace AM, Lacitignola L, et al. Respiratory effects of low versus high tidal volume with or without positive end-expiratory pressure in anesthetized dogs with healthy lungs. *Am J Vet Res.* (2018) 79:496–504. doi: 10.2460/ajvr.79.5.496
- Hurtado DE, Villaruel N, Retamal J, Bugeado G, Bruhn A. Improving the accuracy of registration-based biomechanical analysis: a finite element approach to lung regional strain quantification. *IEEE Trans Med Imaging.* (2016) 35:580–8. doi: 10.1109/TMI.2015.2483744
- Retamal J, Hurtado D, Villaruel N, Bruhn A, Bugeado G, Amato MBP, et al. Does regional lung strain correlate with regional inflammation in acute respiratory distress syndrome during nonprotective ventilation? An Experimental Porcine Study. *Crit Care Med.* (2018) 46:e591–e9. doi: 10.1097/CCM.0000000000003072
- Mauri T, Yoshida T, Bellani G, Goligher EC, Carteaux G, Rittayamai N, et al. Esophageal and transpulmonary pressure in the clinical setting: meaning, usefulness and perspectives. *Intensive Care Med.* (2016) 42:1360–73. doi: 10.1007/s00134-016-4400-x
- Araos J, Lacitignola L, Acquafredda C, DiBella C, Stabile M, Guacci E, et al. Definition and clinical evaluation of a recruiting airway pressure based on the specific lung elastance in anesthetized dogs. *Vet Anaesth Analg.* (2021) 48:484–92. doi: 10.1016/j.vaa.2021.03.005
- Persson P, Stenqvist O, Lundin S. Evaluation of lung and chest wall mechanics during anaesthesia using the PEEP-step method. *Br J Anaesth.* (2018) 120:860–7. doi: 10.1016/j.bja.2017.11.076
- Kaminsky DA. What does airway resistance tell us about lung function? *Respir Care.* (2012) 57:85–96; discussion 96–89. doi: 10.4187/respcare.01411
- Bennett FM, Tenney SM. Comparative mechanics of mammalian respiratory system. *Respir Physiol.* (1982) 49:131–40. doi: 10.1016/0034-5687(82)90069-X
- Ranieri VM, Zhang H, Mascia L, Aubin M, Lin CY, Mullen JB, et al. Pressure-time curve predicts minimally injurious ventilatory strategy in an isolated rat lung model. *Anesthesiology.* (2000) 93:1320–8. doi: 10.1097/0000542-200011000-00027
- Ferrando C, Suarez-Sipmann F, Gutierrez A, Tusman G, Carbonell J, Garcia M, et al. Adjusting tidal volume to stress index in an open lung condition optimizes ventilation and prevents overdistension in an experimental model of lung injury and reduced chest wall compliance. *Crit Care.* (2015) 19:9. doi: 10.1186/s13054-014-0726-3
- Corcoran BM. Static respiratory compliance in normal dogs. *J Small Anim Pract.* (1991) 32:438–42. doi: 10.1111/j.1748-5827.1991.tb00981.x
- Grassi L, Kacmarek R, Berra L. Ventilatory mechanics in the patient with obesity. *Anesthesiology.* (2020) 132:1246–56. doi: 10.1097/ALN.0000000000003154
- Watson RA, Pride NB. Postural changes in lung volumes and respiratory resistance in subjects with obesity. *J Appl Physiol.* (1985). (2005) 98:512–7. doi: 10.1152/jappphysiol.00430.2004
- Magnusson L, Spahn DR. New concepts of atelectasis during general anaesthesia. *Br J Anaesth.* (2003) 91:61–72. doi: 10.1093/bja/aeg085
- Neto AS, Hemmes SN, Barbas CS, Beiderlinden M, Fernandez-Bustamante A, Futier E, et al. Association between driving pressure and development of postoperative pulmonary complications in patients undergoing mechanical

- ventilation for general anaesthesia: a meta-analysis of individual patient data. *Lancet Respir Med.* (2016) 4:272–80. doi: 10.1016/S2213-2600(16)00057-6
30. Mazzinari G, Serpa Neto A, Hemmes SNT, Hedenstierna G, Jaber S, Hiesmayr M, et al. The Association of Intraoperative driving pressure with postoperative pulmonary complications in open versus closed abdominal surgery patients - a posthoc propensity score-weighted cohort analysis of the LAS VEGAS study. *BMC Anesthesiol.* (2021) 21:84. doi: 10.1186/s12871-021-01268-y
 31. Wellman TJ, Winkler T, Costa EL, Musch G, Harris RS, Zheng H, et al. Effect of local tidal lung strain on inflammation in normal and lipopolysaccharide-exposed sheep*. *Crit Care Med.* (2014) 42:e491–e500. doi: 10.1097/CCM.0000000000000346
 32. Motta-Ribeiro G, Winkler T, Hashimoto S, Vidal Melo MF. Spatial heterogeneity of lung strain and aeration and regional inflammation during early lung injury assessed with PET/CT. *Acad Radiol.* (2019) 26:313–25. doi: 10.1016/j.acra.2018.02.028
 33. Lagier D, Vidal Melo MF. Protective ventilation during surgery: do lower tidal volumes really matter? *Anaesth Crit Care Pain Med.* (2021) 40:100807. doi: 10.1016/j.accpm.2021.100807
 34. Protti A, Cressoni M, Santini A, Langer T, Mietto C, Febres D, et al. Lung stress and strain during mechanical ventilation: any safe threshold? *Am J Respir Crit Care Med.* (2011) 183:1354–62. doi: 10.1164/rccm.201010-1757OC
 35. Bruhn A, Bugeo D, Riquelme F, Varas J, Retamal J, Besa C, et al. Tidal volume is a major determinant of cyclic recruitment-derecruitment in acute respiratory distress syndrome. *Minerva Anesthesiol.* (2011) 77:418–26.
 36. Pasticci I, Cadringer P, Giosa L, Umbrello M, Formenti P, Macri M. Determinants of the esophageal-pleural pressure relationship in humans. *J Appl Physiol.* (2020) 128:78–86. doi: 10.1152/jappphysiol.00587.2019
 37. Petersson J, Glenny RW. Gas exchange and ventilation-perfusion relationships in the lung. *Eur Respir J.* (2014) 44:1023–41. doi: 10.1183/09031936.00037014
 38. Staffieri F, Franchini D, Carella GL, Montanaro MG, Valentini V, Driessen B, et al. Computed tomographic analysis of the effects of two inspired oxygen concentrations on pulmonary aeration in anesthetized and mechanically ventilated dogs. *Am J Vet Res.* (2007) 68:925–31. doi: 10.2460/ajvr.68.9.925
 39. Martin-Flores M, Tseng CT, Robillard SD, Abrams BE, Campoy L, Harvey HJ, et al. Effects of two fractions of inspired oxygen during anesthesia on early postanesthesia oxygenation in healthy dogs. *Am J Vet Res.* (2018) 79:147–53. doi: 10.2460/ajvr.79.2.147
 40. Martin-Flores M, Cannarozzo CJ, Tseng CT, Lorenzutti AM, Araos JD, Harvey HJ, et al. Postoperative oxygenation in healthy dogs following mechanical ventilation with fractions of inspired oxygen of 0.4 or >0.9. *Vet Anaesth Analg.* (2020) 47:295–300. doi: 10.1016/j.vaa.2020.01.002
 41. Yoshida T, Amato MBP, Grieco DL, Chen L, Lima CAS, Roldan R, et al. Esophageal manometry and regional transpulmonary pressure in lung injury. *Am J Respir Crit Care Med.* (2018) 197:1018–26. doi: 10.1164/rccm.201709-1806OC
- Conflict of Interest:** The authors declare that the research was conducted in the absence of any commercial or financial relationships that could be construed as a potential conflict of interest.
- Publisher's Note:** All claims expressed in this article are solely those of the authors and do not necessarily represent those of their affiliated organizations, or those of the publisher, the editors and the reviewers. Any product that may be evaluated in this article, or claim that may be made by its manufacturer, is not guaranteed or endorsed by the publisher.
- Copyright © 2021 Araos, Lacitignola, de Monte, Stabile, Porter, Hurtado, Perez, Crovace, Grasso, Martin-Flores and Staffieri. This is an open-access article distributed under the terms of the Creative Commons Attribution License (CC BY). The use, distribution or reproduction in other forums is permitted, provided the original author(s) and the copyright owner(s) are credited and that the original publication in this journal is cited, in accordance with accepted academic practice. No use, distribution or reproduction is permitted which does not comply with these terms.